**First European Conference on Earthquake Engineering and Seismology**
(a joint event of the 13th ECEE & 30th General Assembly of the ESC)
**Geneva, Switzerland, 3-8 September 2006**
**Paper Number: 274**

# HYSTERETIC ENERGY DISSIPATION IN LATERALLY RESTRAINED STEEL TUBE AND SOLID BAR BRACES

**Oguz C. CELIK[1], Jeffrey W. BERMAN[2] and Michel BRUNEAU[3]**

## SUMMARY

This paper describes an experimental investigation into the seismic behavior and efficiency of steel frames with special bracing infills. Cold formed steel studs (CFSS), typically used in nonstructural partition walls, were studied to determine if they could be used to laterally restrain braces against buckling and thus enhance their seismic performance. Four specimens were ductile designed and then tested under cyclic loading. Specimens have either single diagonal tube or solid bar X braces with and without CFSS and U brackets providing out-of-plane and in-plane buckling restraint respectively. Behavioral characteristics of the specimens are quantified with an emphasis on hysteretic energy dissipation. Experimental results show that, at the same ductility levels, the cumulative energy dissipation of braces can be significantly increased when CFSS members are used. However, when tubular cross sections are used for braces, local buckling led to a reduced fracture life compared to the case without CFSS members. CFSS members appear to be relatively more effective when solid bar braces having large slenderness (tension-only braces) are used, since the difference between dissipated energies obtained with and without studs is substantial.

## 1. INTRODUCTION

Hysteretic behavior of concentrically braced steel frames (CBF), as a system, highly depends on the hysteretic behavior of bracing members. Hysteretic loops of an axially loaded brace subject to buckling are usually unsymmetrical with degradation of the buckling strength and hysteretic energy dissipation in compression in each subsequent cycle.

Many past and recent studies [e.g. Black et al. 1980, Ikeda and Mahin 1984, Tremblay 2002, and Lee and Bruneau 2002] have revealed that a substantial amount of cumulative energy can be dissipated in steel braces in the post buckling range when those members are subjected to reversed cyclic displacements. Zayas et al. [1980] experimentally demonstrated that pipe braces with lower effective slenderness ($KL/r$) and diameter-to-wall thickness ($D/t$) ratios performed better, exhibiting fuller hysteretic loops, less strength degradation, and greater resistance to local buckling. The efficiency of energy dissipation decreased rapidly after local buckling. Ikeda and Mahin [1984] recommended the use of stocky braces over slender braces. As a result of such studies, codes require that stocky braces be used in seismically active regions. More recent research has recognized that the benefits of using braces having low slenderness ratios are somewhat offset by lower fracture life that results from the local buckling that may develop in stocky braces. Both Tremblay [2002] and Lee and Bruneau [2002] reported and quantified the degradation of compressive strength and hysteretic energy dissipation, and modified fracture life equations previously proposed by Lee and Goel [1987]. In parallel, other researchers [Filiatrault and Tremblay, 1998] have advocated the use of tension-only braces in seismic applications, to overcome some of

[1] Assoc.Prof., Istanbul Tech. University, Faculty of Architecture, Div. of Theory of Structures, Taskisla, Taksim, 34437, Istanbul, Turkey. Email : celikoguz@itu.edu.tr
[2] Dr., Post-Doctoral Research Associate, Department of CSEE, University at Buffalo, Amherst, NY 14260, USA. Email: jwberman@eng.buffalo.edu
[3] Director, MCEER, Prof., Department of CSEE, University at Buffalo, Amherst, NY 14260, USA. Email: bruneau@buffalo.edu

these problems, while recognizing that this system is possibly limited in applications for a number of reasons [Bruneau et al. 1998].

Ideally, in the perspective of seismic design, it is desirable to delay (or possibly prevent) global and local buckling of braces in steel frames [Iwata et al., 2000]. To improve the hysteretic characteristics of CBF braces, cold-formed steel studs (CFSS) of the type often used in non-structural partition walls could be specifically designed to laterally restrain braces against buckling and enhance their seismic performance. This would require special design of CFSS members to elastically resist the out-of-plane forces developing at the onset of brace buckling. To investigate the validity of such a solution (i.e. whether CFSS wall units could be designed to achieve the above objective, how effective they are in improving hysteretic behavior), four specimens have been designed and cyclically tested. Single square tube braces and rectangular solid bar X braces with and without CFSS members were tested under quasi-static cyclic displacement histories.

This paper reports on the cyclic inelastic behavior of proposed, moveable steel bracing infills for steel framed buildings. The obtained strengths, stiffnesses, maximum displacement ductilities, and cumulative energy dissipation capacities are compared. Note that the infill types considered in this study could be implemented in new buildings or as a retrofitting technique in seismically vulnerable buildings lacking of strength, lateral stiffness, or ductility.

## 2. SOME REMARKS ON CURRENT CODES

Significant research on the behavior of steel braces was conducted in the 1970s and 1980s. Many code provisions, details and limitations until the early 1990s were based on these studies. Since the hysteretic loops for CBF were less ideal with observed pinching due to a progressive strength degradation upon repeated buckling of the compression brace (especially in tension-only braced frames), CBF were assigned response modification factors (R) on the order of 75% of what were assumed for moment frames in the USA. This contributed to the wide-spread use of moment frames in areas of high seismicity. However, from 1992 to date, the design requirements for CBF in the AISC Seismic Provisions [AISC, 2002] have evolved. In the 1997 edition, a new category CBF was introduced as special concentrically braced frames (SCBF) on the basis that CBF could exhibit ductile and stable hysteretic behavior with adequate energy dissipation during cyclic inelastic buckling if ductile detailing was provided. Higher R values were assigned for SCBF (20% higher than for ordinary CBF). Some relaxations on the maximum brace slenderness ratio permitted for SCBF were also introduced. However, emphasis on promoting stocky braces over slender braces still remains despite the fact that the fracture life of stocky braces is known to be generally less than for slender braces. Based on the current codes, earthquake resistant design requirements for CBF are reviewed in [Celik et al., 2004].

## 3. DUCTILE DESIGN OF SPECIMENS

### 3.1 Boundary Frames

The boundary frame dimensions were selected to be representative of bay dimensions for frames located in a test-bed structure called the “MCEER Demonstration Hospital” [Yang and Whittaker, 2002]. The boundary frame with an aspect ratio ($L/h$) of 2.0 is taken from that hospital’s structural system, where $L$ and $h$ are the bay width and the height of the specimen respectively, but actual scale of the boundary frame is 1/2 of the prototype due to limitations of the testing apparatus. However, full scale systems would behave similarly to those tested, and deliver the same cyclic inelastic performance provided the braces have the same member slenderness, and CFSS’ stiffness and strength are designed per the procedure described in [Celik et al., 2005]. Two boundary frames were used for the specimens. All the beam and column dimensions, as well as connection angles, were kept constant from specimen to specimen to allow a more uniform comparison of the strength, stiffness and seismic energy dissipation capacity of the different proposed retrofit designs. All details related to the boundary frames can be found in [Celik et al., 2004].

### 3.2 Moveable Bracing Infills

Four specimens were designed and constructed using tube and solid bar concentric braces. Two of the specimens had closely spaced vertical cold-formed steel studs introduced to reduce the buckling length of the braces,

approaching to some degree (but not perfectly) the philosophy of buckling-restrained braced frames. All specimens were designed in accordance with the AISC Seismic Provisions [AISC, 2002], AISC LRFD Specifications [AISC, 1999], and AISI [1996] codes as appropriate. These specimens are:

- Specimen F1: CBF with single tube brace and vertical CFSS
- Specimen F2: CBF with single tube brace and without vertical CFSS
- Specimen F3: CBF with solid rectangular X braces and vertical CFSS
- Specimen F4: CBF with solid rectangular X braces and without vertical CFSS

In Specimens F1 and F3, CFSS members were spaced at 457.2mm (18in.) center-to-center. All specimens were tested in the University at Buffalo's Structural Engineering and Earthquake Simulation Laboratory (SEESL). A typical test set-up for the specimens is shown in Figure 1. The above choice of specimens made it possible to compare the seismic energy dissipation behavior of frames with either slender or stocky brace members, the latter achieved by the presence of the studs providing intermediate lateral supports both in the in-plane and out-of-plane directions and thus reducing the effective slenderness of the braces in both directions. The vertical CFSS were installed on both sides of the braces and were connected to them without bolting through the braces (to eliminate the possibility of net section fracture). The intended result was more stable, less pinched hysteretic loops with less stiffness and strength degradation under cyclic loading.

Since the fracture life of tube braces may be reduced significantly due to local buckling effects, one could question the usefulness of preventing global buckling of tubular braces. Specimens F1 and F2 allow a comparison of the fracture life of tube brace systems having low and high effective slenderness ratios.

### 3.3 Materials

ASTM A572 Gr.50 steel was used for the boundary frame. Locally available, 12 gauge, 228 MPa (33 ksi) yield point CFSS products were used in this research [Dietrich Product Data, 2001]. The solid bar braces, gussets and angle connectors for the studs were also ASTM A572 Gr.50. U brackets used as in-plane buckling restrainers, were ASTM A36 grade steel. The tube material was ASTM A500 Gr.B with minimum yield stress of 317 MPa (46 ksi). Bolts used are A490 grade in gussets-to-boundary-frame connections, and A307 grade for all other connections of the infills. ASTM Standard coupon tests [ASTM, 2002] gave average values of yield stresses of 377 MPa for solid braces and 385 MPa for the tubes. The yield strength of the tube brace coupons was calculated using a 0.2% strain offset, since this steel exhibited no definite yield plateau. The solid bar coupons had an elastic-plastic behavior. Prior to testing, these material data were used in static pushover analyses of the specimens conducted using SAP2000 [CSI, 1998] to predict the load-displacement curves of the specimens.

## 4. SPECIMENS

Double web-angle beam-to-column connections were welded to the beam web using typical 8mm fillet welds all around the angle legs. Connection to the column flanges used six 31.75mm (1¼") diameter A490 bolts. Column bases were connected to clevises via endplates which were welded to the columns and bolted to the clevises. Further details regarding the specimens can be found in [Celik et al., 2004].

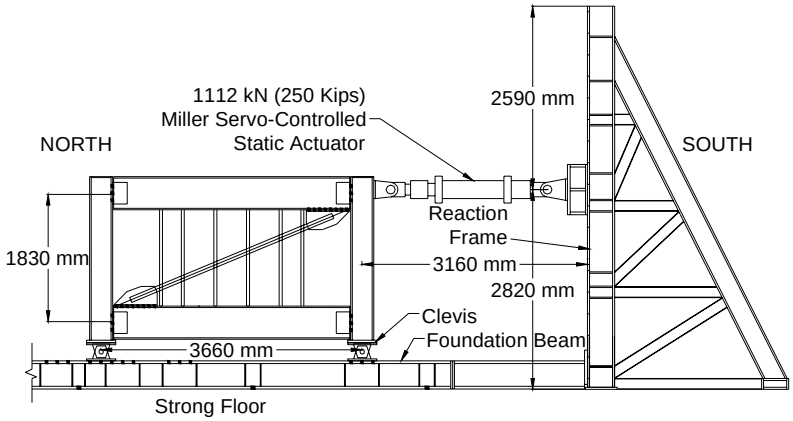


**Figure 1: Typical test set-up for specimens**

Braces were designed to be the largest possible that could be tested without exceeding the maximum force capacity of 1112kN (250Kips) of the largest actuator available in the laboratory, with a safety factor of 1.50, and taking strain hardening effects into account. As a result, single tube brace of 76.2mm by 76.2mm (3in.x3in.) with t=7.94mm (5/16in.) wall thickness, and solid bar X braces having a cross section of 25.4mm by 50.8mm (1in.x2in.), were selected. Specimens F1 to F4 are illustrated in Figures 2a to 2d respectively.

Cold-formed steel studs used in Specimen F1 and Specimen F3 were 5½" CSJ 12 gauge by Dietrich [2001]. Nuts for the bolts used in stud-to-angle, angle-to-beam, and stud-to-stud connections were in the snug-tight condition. U brackets used as in-plane buckling restrainers were custom made. The distinctive feature of the connection detail around the brace and CFSS intersection region is that there is no mechanical connection to the braces. CFSS members are connected to each other via their inner flanges using a long, 12.7mm diameter bolt passing through the holes on the brackets. U brackets and CFSS members were to be in perfect contact with the brace surfaces to provide a direct load transfer. Small spacers having the same section of the bar brace were used in Specimen F3 to fill the gap in the connection.

## 5. CYCLIC TESTING AND OBSERVATIONS

Each specimen was subjected to quasi-static cyclic loading in accordance with the ATC-24 [1992] protocol. Since the top horizontal displacement of the specimens is directly related to the brace axial displacement, this horizontal value was taken as the displacement control parameter for all tests. As the study of cyclic inelastic buckling behavior of the brace elements was the objective of this study, special care was taken during the tests to identify the point of buckling initiation for the braces. In Specimen F1, in which the tension yield and buckling strengths of the brace were close to each other, the load was first applied to have tension in the brace, and in the above procedure, the experimentally obtained $\delta_y$ (specimen top horizontal displacement at the onset of brace tension yielding) was taken as the test control parameter. To facilitate comparison between the results obtained for Specimens F1 and F2 in subsequent sections, the same cyclic displacement history that was applied to Specimen F1 (i.e. absolute displacement values) was applied to Specimen F2. On the contrary, in Specimen F3 in which tension yield and buckling strengths of the restrained X braces were significantly different from each other, with buckling occurring first, in the above procedure, the experimentally obtained $\delta_b$ (specimen top horizontal displacement at the onset of brace buckling) was taken as the test control parameter. Again, to facilitate comparisons between Specimens F3 and F4, the same cyclic displacement history that was applied to Specimen F3 was applied to Specimen F4.

Yield and buckling values of specimen's forces and displacements were analytically estimated by static pushover analysis using SAP2000, and were used to initially control the tests. However, the experimentally obtained values were used as test control parameters beyond the elastic range. These were determined at the onset of visible nonlinearity in the force-displacement curve, or by the point from which the actuator force tended to drop abruptly (during buckling). The magnitude of the cyclic displacement histories of the specimens are presented in detail in [Celik et al., 2004].

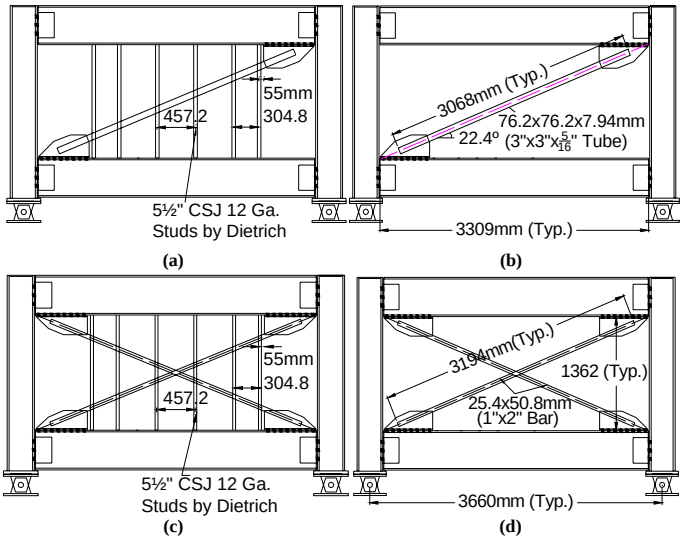


**Figure 2: Schematic of specimens: (a) F1; (b) F2; (c) F3; (d) F4**

The behavior of each specimen, both in the elastic and inelastic ranges, is discussed below. In all cases, experimental base shear force versus drift hysteresis curves are shown in Figure 3, and results for the case of infill only (i.e. after subtracting the contribution of the bare frame) are illustrated in Figure 4. The procedure used to model and subtract the bare frame contribution is evaluated later.

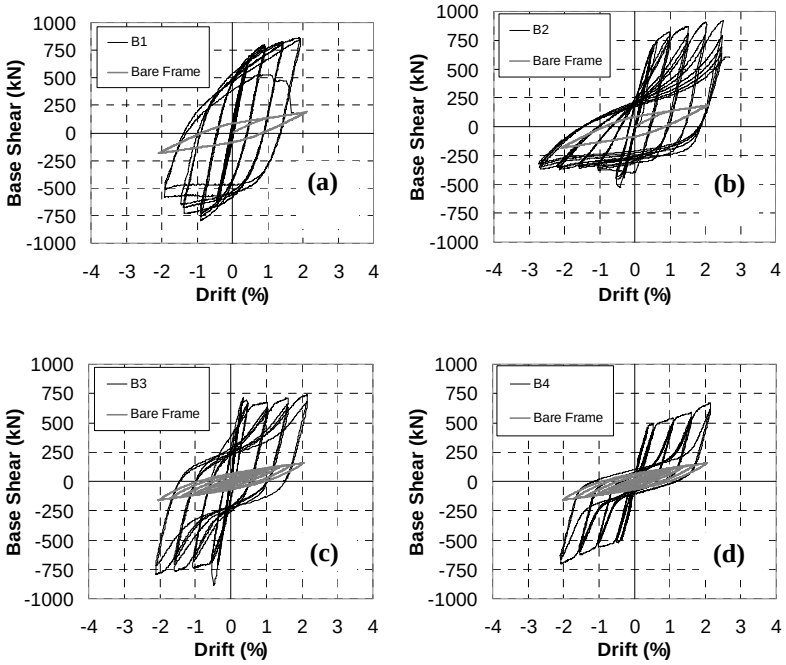


**Figure 3: Experimental hysteresis curves for specimens: (a) F1; (b) F2; (c) F3; (d) F4**

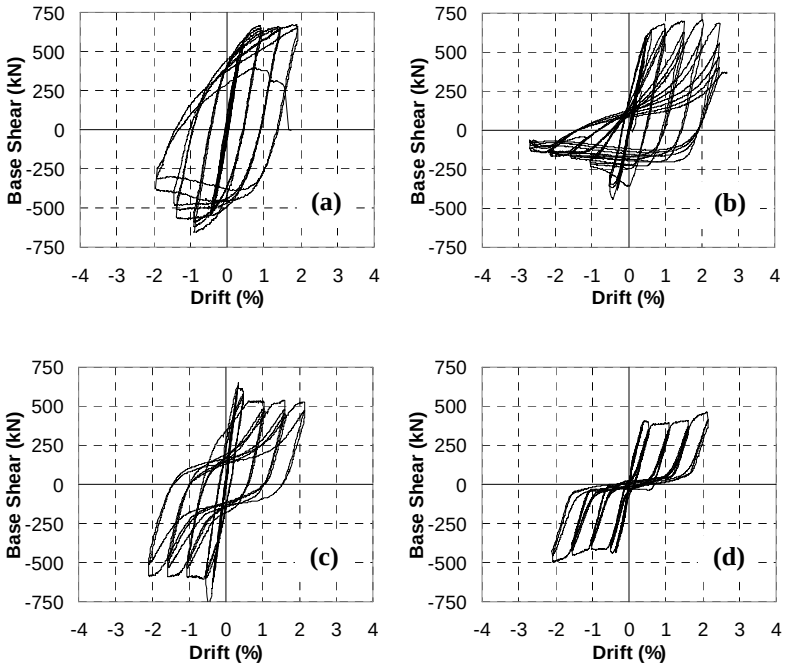


**Figure 4: Comparison of base shear versus drift hysteresis curves for infills: (a) F1 (*KL*/*r*=19.7); (b) F2 (*KL*/*r*=77.3); (c) F3 (*KL*/*r*=65.5); (d) F4 (*KL*/*r*=195.7)**

### 5.1 Specimen F1

Up to 0.96% drift ($2\delta_y$), the specimen did not show significant deterioration in strength and stiffness, in other words, the behavior was almost cyclic symmetric. Beyond this drift level, the shape of the hysteresis curves for Specimen F1 gradually became one-sided upon repeated inelastic buckling of the tubular brace member. However, the difference between the buckling and tension strengths in each cycle was still significantly less than would be expected in absence of lateral bracing by the studs. At 1.44% drift ($3\delta_y$), a decrease in buckling strength was observed due to the development of local buckling in the tube. On the tension side, as expected from the coupon tests, strength increased at each displacement cycle until fracture started to develop. The ratio of the maximum achieved base shear (brace in tension) to the yield base shear is 1.32. Deterioration of the brace post buckling resistance at various drift levels was relatively slow. During the first excursions of compression cycles at 0.96%, 1.44%, and 1.92% drifts, the ratio of the compression strength at that cycle to the peak compression strength reached during the test dropped to 1.00, 0.93, and 0.74. Ratios at the same drift levels for the infill only case are 1.00, 0.87, and 0.60. Strain gauge data showed that 2% strain was reached in the brace at 1.92% drift. A displacement ductility ratio ($\mu$) of 4 was achieved when the tension and compression strengths of the specimen were, respectively, 100% and 67% of the maximum values obtained experimentally. As seen from Table 1, the contribution of the infill to the initial stiffness is 88%. The elastic experimental effective length factor ($K$) was calculated to be 1.08, compared to a theoretical value of 1.00 (taking $L$ as the diagonal distance between stud centers). This value has been obtained using the measured tube strain gauge data, at axial strains below the yield level, to calculate the bending moment diagram on the brace; the maximum of the distances between two successive inflection points on the deflected shape (points of zero moment on the bending moment diagram) was taken as the effective length of the brace. Fuller hysteretic loops indicate that the contribution of the brace in compression to the total energy dissipation is substantial.

**Table 1: Behavioral characteristics of tested specimens**

| Specimen | Total Initial Stiffness (kN/mm) | Initial Stiffness-Infill (kN/mm) | Yield or Buckling Base Shear (kN) | Yield or Buckling Disp. (mm) | Max. Drift (%) | $\mu$ | $\frac{K_{exp}}{K_{theoretical}}$ | Total Energy (kN.m) | Infill Energy (kN.m) |
|---|---|---|---|---|---|---|---|---|---|
| F1 | 88.8 | 78.2 | 636.1 | 11.4 | 1.92 | 4 | 1.08 | 274 | 227 |
| F2 | 61.4 | 51.0 | 511.5 | 10.2 | 2.88 | 6* | 1.81*** | 310 | 192 |
| F3 | 136.0 | 125.7 | 898.5 | 11.9 | 2.16 | 4 | 0.97 | 205 | 169 |
| F4 | 106.6 | 96.3 | 182.4 | 3.0 | 2.16 | 4** | 1.25 | 95 | 37 |

* Reached displacement ductility based on the yield displacement of Specimen F1.
** Reached displacement ductility based on the buckling displacement of Specimen F3.
*** This difference comes from the increase in the brace clear length due to inelastic gusset behavior.

The out-of-plane buckling mode of the brace (Cycle 16, - $4\delta_y$), development of local buckling in middle brace segment (Cycle 16, - $4\delta_y$) and fracture of tube brace middle section (Cycle 18, + $4\delta_y$) are shown in Figure 5.

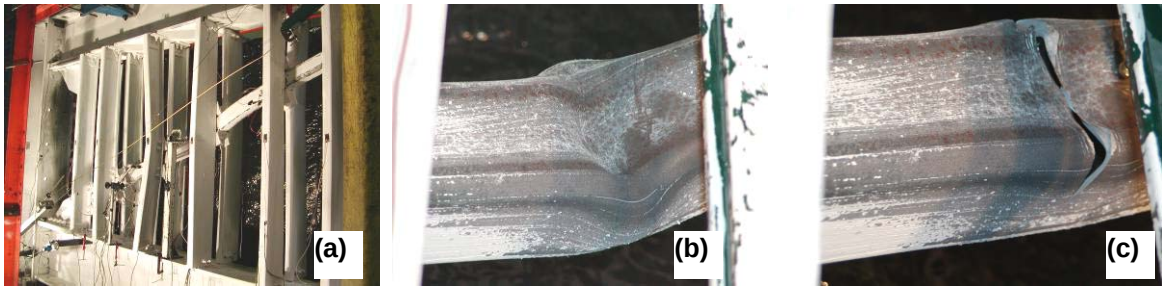


**Figure 5: Damage level in Specimen F1: (a) Out-of-plane buckling mode (Cycle 16, - $4\delta_y$); (b) Development of local buckling in middle brace segment (Cycle 16, - $4\delta_y$); (c) Fracture of tube brace middle section (Cycle 18, + $4\delta_y$)**

### 5.2 Specimen F2

Specimen F2 was subjected to the same displacement history as Specimen F1 to facilitate comparison of the relative hysteretic energy dissipation capacity of the two specimens. However, additional cycles were performed

for Specimen F2 beyond the maximum displacements reached for Specimen F1, until failure, to allow determination of the fracture life of the tube brace. Specimen F2 exhibited ductile and stable cyclic behavior up to 2.40% drift, although some pinching is obvious in the hystereses. Up to 0.48% drift, the hysteresis curves are cyclic symmetric, however, in the aftermath of brace buckling, they become one-sided due to the deterioration in buckling strength. On the tension side, strength increases until fracture develops. The ratio of the maximum tension strength to the yield strength is 1.26. During the first excursions of compression cycles at 0.48%, 0.96%, 1.44%, 1.92%, and 2.40% drifts, the ratio of the compression strength at that cycle to the peak compression strength reached during the test dropped to 1.00, 0.76, 0.58, 0.46, and 0.44. For the infill-only case, ratios at the same drifts were 1.00, 0.82, 0.53, 0.47, and 0.46. Strain gauge data showed that 1.5% strain was reached in the tubular brace at 2.50% drift. Specimen F2 exhibited a displacement ductility ratio ($\mu$) of 6, when the tension and compression strengths were 65% and 46% of the maximum achieved peak strengths.

Table 1 shows that the contribution of the brace to the initial stiffness is 83%. The experimental elastic *K* factor was found to be 0.90 compared to a theoretical value of 0.5 (taking *L* as the clear brace length between gussets). A general view of the buckled brace (Cycle 21, $-5\delta_y$) is shown in Figure 6a.

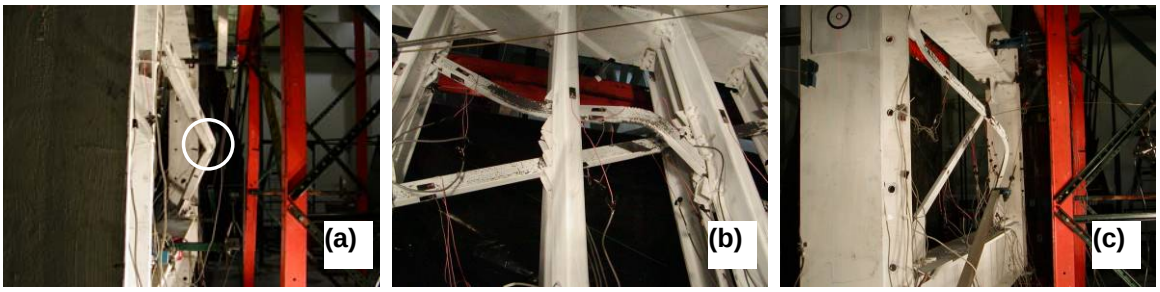


**Figure 6: Damage level in specimens: (a) F2 ($-5\delta_y$, Cycle 21); (b) F3 ($-4\delta_y$, Cycle 19); (c) F4 ($-4\delta_y$, Cycle 19)**

### *5.2.1 Fracture life of Specimens F1 and F2*

Experimental fracture life ($\Delta_{f,exp}$) of tube braces can be obtained from hysteretic curves following the procedure proposed by Lee and Goel [1987]. In this procedure, hysteresis curves are normalized by yield strength and the corresponding yield displacement. Next, the tension branch of the hysteresis is divided into two regions, $\Delta_1$ and $\Delta_2$, defined at 1/3 of the yield strength. $\Delta_1$ is the tension deformation from the load reversal point to 1/3 of the yield strength point displacement, while $\Delta_2$ is from 1/3 yield strength point to the unloading point. Experimental fracture life is then calculated using

$$\Delta_{f,exp} = \sum\left(0.1\Delta_1 + \Delta_2\right) \tag{1}$$

Experimental values of $\Delta_{f,exp}$=32.9 and 64.7 were found for Specimens F1 and F2 respectively. Theoretical fracture lives ($\Delta_f$) introduced in Lee and Goel [1987] and Archambault et al. [1995] methods were also calculated. The Lee and Goel Model is given by:

$$\Delta_f = C_s \frac{(46/F_y)^{1.2}}{[(b-2t)/t]^{1.6}}\left(\frac{4b/d+1}{5}\right) \tag{2}$$

where $C_s$=1560 (a numerical constant), $F_y$= yield stress (ksi), b=gross width of section, d=gross depth of section and t=thickness of section, and the Archambault et al. Model is given by:

$$\Delta_f = C_s \frac{(317/F_y)^{1.2}}{[(b-2t)/t]^{0.5}}\left(\frac{4b/d+1}{5}\right)^{0.8} \times (70)^2 \quad \text{for} \quad KL/r < 70 \tag{3a}$$

$$\Delta_f = C_s \frac{(317/F_y)^{1.2}}{[(b-2t)/t]^{0.5}}\left(\frac{4b/d+1}{5}\right)^{0.8} \times (KL/r)^2 \quad \text{for} \quad KL/r \geq 70 \tag{3b}$$

where $C_s$ = 0.0257, where all other parameters are as defined above but $F_y$ is in MPa.

Numerical values of $\Delta_f$=48.2 and 36.1 were obtained for the Lee and Goel and the Archambault et al. methods respectively for Specimen F1, and 48.2 and 43.9 for Specimen F2, using the experimental *K* values. The ratios of the experimental to theoretical values for these two models are 0.68 and 0.91 for Specimen F1, and 1.34 and 1.47 for Specimen F2. For Specimen F1, the Archambault et al. method agrees reasonably well with the experimental one. For Specimen F2, both methods underestimate the fracture life of the tube brace, and the Lee and Goel model gives closer results in this case.

### 5.3 Specimen F3

Up to approximately 0.50% drift, the specimen did not show deterioration in strength and stiffness. At the onset of buckling of the east side brace segment between the fourth and the fifth studs (counting from the north), the base shear dropped abruptly. After buckling, the hysteresis for Specimen F3 stabilized and fuller curves on both tension and compression sides developed. For negative and positive base shears, absolute ratios of the maximum negative and positive base shears at final cycles to the peak base shear at brace buckling are 0.89 and 0.83 respectively. The overall behavior of Specimen F3 was ductile and stable up to 2.16% drift, although pinching in the hysteretic loops is apparent. During the first excursions of compression cycles, the ratio of the negative base shear (total specimen) at that cycle to the negative peak base shear at 0.54%, 1.08%, 1.62%, and 2.16% drifts dropped to 1.00, 0.83, 0.85, and 0.89. For the infill-only case, same ratios were 1.00, 0.75, 0.73, and 0.73. Strain gauge data showed that the bar braces exhibited stable energy dissipation up to 2.16% drift, producing about 3% maximum strain (including axial and bending effects) in the mid-length of the east side brace. A displacement ductility ratio ($\mu$) of 4 was achieved without any significant strength and stiffness degradation with the exception of initial buckling values. Table 1 indicates the substantial increase in stiffness for this specimen. The contribution of the infill to the initial stiffness is 92%. Furthermore, an experimental elastic effective length factor (*K*) of 0.97 was obtained. Yielding of braces (Cycle 19, $-4\delta_y$) is depicted in Figure 6b.

### 5.4 Specimen F4

The hysteresis for Specimen F4 is fairly symmetrical in the elastic and inelastic cycles. The overall behavior of Specimen F4 was ductile and stable up to 2.16% drift, although significant pinching is visible in the hystereses. The infill hysteresis exhibits near elastic-plastic behavior (during each excursion) up to the application of the last cycle (2.16% drift). The ratio of the maximum tension strength to the strength at the displacement level of Specimen F3 buckling is 1.28. During the first excursions of each imposed drift level, the ratio of the maximum positive and negative base shear during that cycle to the strength at buckling at 0.54%, 1.08%, 1.62%, and 2.16% drifts reached 1.00, 1.10, 1.20, and 1.36. For the infill-only case, these ratios were 1.00, 0.98, 1.01, and 1.14. For the negative side of the hystereses, the corresponding ratios were 1.00, 1.07, 1.20, and 1.34 for the total frame, and were 1.00, 0.94, 1.03, and 1.12 for the infill only case. Up to 1.7% strain was reached in the bar braces at 2.16% drift. Specimen F4 exhibited a displacement ductility ratio ($\mu$) of 4. Table 1 (presented earlier) shows that the contribution of the bar braces to initial stiffness is about 90%. An experimental elastic *K* factor of 0.63 was found. A general view of damage in the specimen (Cycle 19, $-4\delta_y$) is shown in Figure 6c.

### 5.5 Boundary Frame Behavior and Hysteretic Modeling

Cyclic tests were also performed on the bare frames to characterize their hysteretic behavior. The bounding surface model developed by Dafalias and Popov [1976] was used to model the bare frame cyclic behavior. To fit the experimental data, modeling parameters needed to develop the hystereses were calculated. Numerical results showed that the error in the dissipated cumulative energy was less than 10% between the modeled and tested boundary frames. Details on this procedure can be found in Berman and Bruneau [2003] and Celik et al. [2004].

## 6. CUMULATIVE HYSTERETIC ENERGY DISSIPATION AND COMPARISON

Since the cumulative energy dissipation is a useful measure of the seismic efficiency of a structural system, these values were calculated, and the variation of cumulative energy dissipation with cumulative number of cycles are plotted in Figure 7 for the total frame and infill-only cases. Figure 7 and Table 1 show that, for Specimen F1, 83% of the total energy was dissipated by the infill versus 17% for the boundary frame. In Specimen F2, 62% of the total energy was dissipated by the infill versus 38% for the boundary frame. For Specimen F3, 82% of the total energy was dissipated by the infill versus 18% for the boundary frame. For Specimen F4, these numbers are 39% and 61% respectively. Specimen F1 achieved the maximum hysteretic energy dissipation for the infill alone. Percent energy dissipation amounts for other specimens are 85%, 74%, and 16% of Specimen F1 for

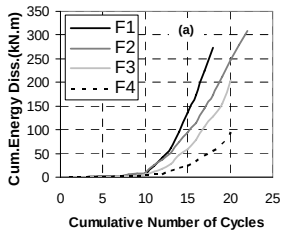


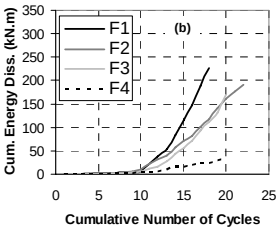


**Figure 7: Comparison of cumulative energy dissipation for specimens: (a) Total frame; (b) Infill**

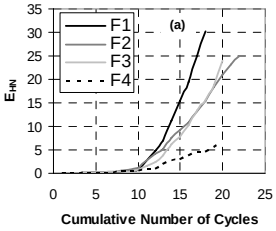


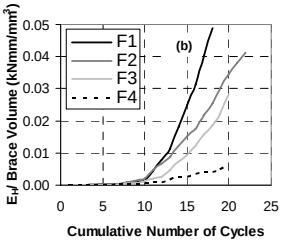


**Figure 8: Infill energy: (a) Normalized (b) Energy dissipation per brace volume used**

Specimens F2, F3, and F4 respectively. Table 1 shows that braces having CFSS members had greater hysteretic energy dissipation. Cumulative hysteretic energy was the greatest in Specimen F1, although this specimen had less maximum displacement ductility due to its lower fracture life as compared to Specimen F2. Specimen F2 dissipated the largest amount of total hysteretic energy, essentially due to its higher fracture life. A displacement ductility of 6 was reached prior to fracture, the largest value for all specimens tested (but Specimens F3 and F4 were not tested up to failure to save the boundary frames). The behavior was ductile and stable. Solid bar braces in Specimen F3 dissipated a relatively moderate amount of energy with ductile but pinched hysteretic curves. CFSS members and U brackets reduced the buckling length of the braces effectively. The least amount of cumulative energy was dissipated by Specimen F4. The hysteresis curves were stable yet significantly pinched, as expected. A displacement ductility of 4 was reached without any visible damage. The maximum drift reached by Specimen F2 was 2.88%. Specimens F1, F3, and F4 exhibited maximum drifts of 1.92%, 2.16%, and 2.16% respectively.

To better compare the effectiveness of each specimen, normalized values of base shear and energy dissipation (infill-only) were calculated and plotted in Figure 8a. Hysteretic energy dissipation was normalized as follows:

$$E_{HN} = \frac{E_H}{V_y \delta_y} \tag{4}$$

where $E_{HN}$=normalized cumulative hysteretic energy dissipation, $E_H$=cumulative hysteretic energy dissipation, $V_y$=yield (or buckling) base shear, and $\delta_y$=experimentally obtained yield or buckling displacement. Normalized energies for Specimens F3 and F4 are less than those for Specimens F1 and F2. Shown in Figure 8b is the variation of volumetric energy dissipation versus cumulative number of cycles. Peak energies of 0.049, 0.041, 0.028, and 0.006 kNmm/mm$^3$ are found for Specimens F1, F2, F3, and F4 respectively. Additionally, at a common ductility of 4, these values become 0.049, 0.025, 0.028, and 0.006 kNmm/mm$^3$, which show that braces having CFSS had better hysteretic energy dissipation capacity.

## 7. CONCLUSIONS

The major conclusions reached from this experimental study are as follows:

1. Specimen F1 (concentrically braced frame with single tube brace and vertical CFSS members) achieved superior behavior over the other specimens in terms of infill cumulative hysteretic energy dissipation at given drift values. Maximum displacement ductilities (μ) attained for Specimens F1 and F2 are 4 and 6, respectively. Experimental fracture life of the tube in F2 was higher than that of the tube in Specimen F1, as reducing the buckling length for tubular cross section braces also accelerated their local buckling.
2. The use of CFSS and U brackets as buckling restrainers was more effective in tension-only braced frames than in tension-compression braced frames. The relative increase in energy dissipation for the tension only systems (i.e., the increase in energy dissipated in Specimen F3 versus Specimen F4) was significantly larger than the relative increase for tension compression systems (i.e., the increase when considering Specimen F1 versus Specimen F2). Solid braces and/or tension only systems may be able to sustain larger amounts of reversed axial cyclic displacements, since local buckling is not likely to occur.
3. Using dissipated hysteretic energy per brace volume to compare the relative effectiveness of these specimens showed that braces having CFSS had better hysteretic energy dissipation capacity.
4. Structural use of CFSS members as out-of-plane buckling restrainers also helped reduce the out-of-plane displacements of braces. This would minimize the wall cladding damages that may occur as a result of large lateral displacements during buckling of braces under severe earthquake excitations.

Performance of CFSS members in Specimen F3 was better than the ones in Specimen F1, which could be attributed to the effect of bracing configurations.

## ACKNOWLEDGMENTS

This research was supported in part by the Earthquake Engineering Research Centers Program of the National Science Foundation (NSF) under Award Number EEC-9701471 to the Multidisciplinary Center for Earthquake Engineering Research (MCEER).

## 8. REFERENCES

AISC (1999), Load and Resistance Factor Design (LRFD) Specification for Structural Steel Buildings, *American Institute of Steel Construction*, Chicago, IL.

AISC (2002), Seismic Provisions for Structural Steel Buildings, *American Institute of Steel Construction*, Chicago, IL.

AISI (1996), Cold-Formed Steel Design Manual, *American Iron and Steel Institute*, Washington, DC.

Archambault, M-H., Tremblay, R. and Filiatrault, A. (1995), Étude du Comportement Séismique des Contreventements Ductiles en X Avec Profilés Tubulaires en Acier, Rapport No. EPM/GCS-1995-09, Département de Génie Civil, Section Structures, *École Polytechnique de Montréal*, Septembre, Québec.

ASTM (2002), Standard Test Methods and Definitions for Mechanical Testing of Steel Products, A 370-97a, *American Society for Testing and Materials*, Philadelphia, PA.

ATC-24 (1992), Guidelines for Cyclic Seismic Testing of Components of Steel Structures, *Applied Technology Council*, California.

Berman, J. W. and Bruneau, M. (2003), Experimental Investigation of Light-Gauge Steel Plate Shear Walls for the Seismic Retrofit of Buildings, Technical Report MCEER-03-0001, *Multidisciplinary Center for Earthquake Engineering Research*, Buffalo, NY.

Black, R.G., Wenger W.A.B. and Popov, E.P. (1980), Inelastic Buckling of Steel Struts under Cyclic Load Reversals, Report No. UCB/EERC-80/40, Berkeley, California.

Bruneau, M., Whittaker, A.S., and Uang, C.M. (1998), Ductile Design of Steel Structures, *McGraw-Hill*, NY.

Celik, O.C., Berman J.W. and Bruneau, M. (2004), Cyclic Testing of Braces Laterally Restrained by Steel Studs to Enhance Performance During Earthquakes, Technical Report MCEER-04-0003, *Multidisciplinary Center for Earthquake Engineering Research*, Buffalo, NY.

Celik, O.C., Berman J.W. and Bruneau, M. (2005), Cyclic Testing of Braces Laterally Restrained by Steel Studs, *Journal of Structural Engineering*, ASCE, 131, n°7, 1114-1124.

CSI (1998), SAP2000 Integrated Finite Element Analysis and Design of Structures- Detailed Tutorial Including Pushover Analysis, Computers and Structures, Inc., Berkeley, California.

Dafalias, Y.F. and Popov, E.P. (1976), Plastic Internal Variables Formalism of Cyclic Plasticity, *Journal of Applied Mechanics*, ASCE, 43, 645-651.

Dietrich Industries, Inc. (2001), Curtain Wall/Light Gage Structural Framing Products, *ICBO* No. 4784P, LA RR No. 25132.

Filiatrault, A., and Tremblay, R. (1998), Design of Tension-Only Concentrically Braced Steel Frames for Seismic Induced Impact Loading, *Engineering Structures*, 20, n°3, 1087-1096.

Ikeda, K. and Mahin, S.A. (1984), A Refined Physical Theory Model for Predicting the Seismic Behavior of Braced Steel Frames, Report No. UCB/EERC-84/12, Berkeley, California.

Iwata, M., Kato, T. and Wada, A. (2000), Buckling-Restrained Braces as Hysteretic Dampers, *3rd International Conference on Behavior of Steel Structures in Seismic Areas (STESSA 2000)*, Montreal, Canada, 33-38.

Lee, K. and Bruneau, M. (2002), Review of Energy Dissipation of Compression Members in Concentrically Braced Frames, Technical Report *MCEER*-02-0005, October, Buffalo, NY.

Lee, S. and Goel, S.C. (1987), Seismic Behavior of Hollow and Concrete-Filled Square Tubular Bracing Members, Report No. UMEE 87-11, December, Department of Civil Engineering, University of Michigan, Ann Arbor, Michigan.

Tremblay, R. (2002), Inelastic Seismic Response of Steel Bracing Members, *Journal of Constructional Steel Research*, 58, 665-701.

Yang, T.Y., and Whittaker, A. (2002), MCEER Demonstration Hospitals-Mathematical Models and Preliminary Results, Technical Report, *Multidisciplinary Center for Earthquake Engineering Research*, University at Buffalo, Buffalo, NY.

Zayas, V.A., Mahin, S.A. and Popov, E.P. (1980), Cyclic Inelastic Behavior of Steel Offshore Structures, Report No. UCB/EERC-80/27, Berkeley, California.